



HAL
open science

Cool flame of methylcyclohexene isomers in a JSR: Formation of aromatic and polyunsaturated hydrocarbons

Zahraa Dbouk, Roland Benoit, Bakr Hoblos, Nesrine Belhadj, Philippe
Dagaut

► **To cite this version:**

Zahraa Dbouk, Roland Benoit, Bakr Hoblos, Nesrine Belhadj, Philippe Dagaut. Cool flame of methylcyclohexene isomers in a JSR: Formation of aromatic and polyunsaturated hydrocarbons. *Fuel*, 2025, 381, pp.133644. 10.1016/j.fuel.2024.133644 . hal-04777356

HAL Id: hal-04777356

<https://hal.science/hal-04777356v1>

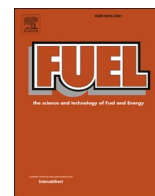
Submitted on 12 Nov 2024

HAL is a multi-disciplinary open access archive for the deposit and dissemination of scientific research documents, whether they are published or not. The documents may come from teaching and research institutions in France or abroad, or from public or private research centers.

L'archive ouverte pluridisciplinaire **HAL**, est destinée au dépôt et à la diffusion de documents scientifiques de niveau recherche, publiés ou non, émanant des établissements d'enseignement et de recherche français ou étrangers, des laboratoires publics ou privés.



Distributed under a Creative Commons Attribution 4.0 International License



Full Length Article

Cool flame of methylcyclohexene isomers in a JSR: Formation of aromatic and polyunsaturated hydrocarbons

Zahraa Dbouk^{a,b}, Roland Benoit^a, Bakr Hoblos^{a,b}, Nesrine Belhadj^{a,b}, Philippe Dagaut^{a,*}^a Centre National de la Recherche Scientifique, I.C.A.R.E.E., Orléans 45071, France^b Université d'Orléans, Avenue de Parc Floral, Orléans 45067, France

ARTICLE INFO

Keywords:

Methylcyclohexene
Cool flame
Oxidation
Jet-stirred reactor
Aromatics
Orbitrap

ABSTRACT

Three isomers of methylcyclohexene were oxidized in a jet-stirred reactor at 10 bar, in fuel-lean conditions (equivalence ratio of 0.5), from 500 to 1150 K. Samples of the reacting mixtures (fuel-oxygen-nitrogen) taken using a sonic fused-silica probe were collected and (i) analyzed by gas chromatography and (ii) for the conditions 620 and 680 K, dissolved in acetonitrile and analyzed by ultra-high performance liquid chromatography and Orbitrap mass spectrometry after direct flow injection or liquid chromatography separation. OH/OD exchange was used by adding D₂O to samples to assess the presence of OH or OOH in products. The reaction with 2,4-dinitrophenylhydrazine allowed the characterizing carbonyl functional groups in the products. A large dataset of oxidation products was observed. Besides highly oxygenated compounds, we observed the production of polyunsaturated and aromatic products in the cool flame oxidation regime. To rationalize the present results, we used chemometric tools, i.e., Van Krevelen plots, calculated oxidation state of carbon, aromaticity index, and aromaticity equivalent index for oxidation products.

1. Introduction

Terpenes, widely emitted by vegetation, are important constituents of volatile organic compounds present in the atmosphere [1]. Since these hydrocarbons have high-energy-density, they represent biofuel candidates [2,3]. However, these chemicals are relatively complex and their combustion mechanism have not been described in the literature. Indeed, to date, the chemical kinetics of combustion of these fuels has not been studied extensively [4–6]. To better characterize the oxidation pathways of these fuels, one could consider simpler model-fuels, such as methylcyclohexene (MCHX) isomers (Table 1).

These cyclic hydrocarbons are produced during the pyrolysis and oxidation of methylcyclohexane [7–9] which has been used as a surrogate component of jet fuels in several works [10,11]. Whereas many studies concern the oxidation of methylcyclohexane, only few have been devoted to the characterization of the oxidation of MCHX isomers. Among them, one can find pyrolysis studies [12–14] and oxidation studies [15–19]. Gulati and Walker studied the oxidation of cyclohexane at 480 °C and 500 Torr total pressure [20]. They reported the formation of benzene among the oxidation products. Moreover, the formation of benzene via the oxidation of cyclohexane, cyclohexene, and 1,3-

cyclohexadiene has been studied by Lemaire et al. in a rapid compression machine under stoichiometric cool-flame conditions and elevated pressure (7 to 14 bar) [21]. They reported selectivity (% C) of 12 % for the conversion of cyclohexene to 1,3-cyclohexadiene and one of 32 % for the formation of benzene via 1,3-cyclohexadiene. We recently reported the formation of aromatic and polyaromatic hydrocarbons during terpenes (limonene and α -pinene) cool flame oxidation [22] in a jet-stirred reactor. Therefore, since MCHXs are considered as surrogate fuels for terpenes, it would be interesting to investigate their oxidation and pay much attention on the formation of aromatic products under cool flame conditions. This is the aim of this work.

Here, we studied experimentally the oxidation of three MCHX isomers in a jet-stirred reactor at 10 bar. In order to observe oxidation products in sufficient quantities, we operated with relatively large initial fuel concentration (3000 ppm), in fuel-lean conditions (equivalence ratio of 0.5), which favors fuel oxidation, and relatively long residence time (2 s). The products of oxidation were analyzed by high-resolution mass spectrometry (HRMS). The large size and complexity of experimental datasets obtained through HRMS analysis require the use chemometric tools to interpret the data. Therefore, Van Krevelen (VK) plots [23], computed oxidation state of carbon [24], aromaticity index [25],

* Corresponding author.

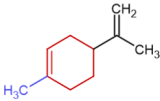
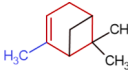
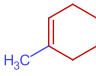
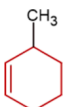
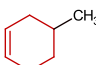
E-mail address: philippe.dagaut@cnrs-orleans.fr (P. Dagaut).<https://doi.org/10.1016/j.fuel.2024.133644>

Received 12 August 2024; Received in revised form 30 October 2024; Accepted 4 November 2024

Available online 12 November 2024

0016-2361/© 2024 The Author(s). Published by Elsevier Ltd. This is an open access article under the CC BY license (<http://creativecommons.org/licenses/by/4.0/>).

Table 1
Chemical structure of monoterpenes and proposed model-fuels.

Monoterpenes (C ₁₀ H ₁₆)	Limonene	
	α-Pinene	
MCHX isomers (C ₇ H ₁₂)	1-Methyl-1-cyclohexene	
	3-methyl-1-cyclohexene	
	4-methyl-1-cyclohexene	

and aromaticity equivalent index [26] were employed.

2. Experimental

2.1. JSR experiments

The present experiments were undertaken in a 42 mL fused silica jet-stirred-reactor (JSR) presented in previous publications [27,28]. The three fuels studied were 1-methyl-1-cyclohexene (>98 % pure, from TCI, CAS 591–49-1), 3-methyl-1-cyclohexene (>93 % pure, from TCI, CAS 591–48-0), and 4-methyl-1-cyclohexene (>98 % pure, from TCI, CAS 591–47-9). As before [29,30] for injecting the fuels, we used a HPLC pump (LC10-AD-VP from Shimadzu) equipped with an online degasser. The three fuels were directed to an in-house vaporizer fed with a flow of nitrogen. Fuel-N₂ (99.95 % pure) and N₂-O₂ (99.995 % pure) were delivered separately to the JSR to circumvent fuel oxidation before entering the reactor. Brooks mass flow meters delivered the N₂ and O₂ flows. A thermocouple (0.1 mm Pt-Pt/Rh-10 % wires), protected by a thin-wall fused silica tube, was moved along the vertical axis of the JSR to confirm thermal homogeneity (typical temperature gradients lower than 1 K/cm). A sonic quartz probe was used to collect gas samples from the JSR. The oxidation of 3000 ppm of fuels in the cool-flame regime was performed at 10 bar, at a mean residence time of 2 s, and in fuel-lean conditions (equivalence ratio $\phi = 0.5$). The JSR temperature was increased stepwise from 500 to 1150 K. See SM for more details.

2.2. Analytical procedures

Gas samples were stored in 1 L Pyrex bulbs for gas chromatography analyses. A flame ionization detector and a quadrupole mass spectrometer were used for quantification and identification, respectively. Besides, they were dissolved into 20 mL of ≥ 99.9 pure acetonitrile (ACN) maintained at 273 K, via 60 min bubbling. We stored these solutions in a freezer at 258 K for the future chemical analyses. Flow injection analyses (FIA) with heated electrospray ionization (HESI) were performed. An Orbitrap Q-Exactive was used to analyze the samples solutions. Several m/z ranges were used for data acquisition in order to improve C-trap transmission sensitivity [31]: 50–750, 150–900, 500–1300, and 900–2000. Only signal $\geq 5 \times 10^3$ counts, way above 'noise' level, were taken into account. Mass calibrations were performed using (+) and (–) HESI calibration mixtures from ThermoScientific. We used a C18 chromatographic column (Luna 1.6 μm , 100 Å, 100x2.1 mm,

from Phenomenex) for reverse-phase ultra-high-performance liquid chromatography (RP-UHPLC) analyses were completed. We eluted 3 μL of liquid samples by a H₂O-ACN mixture at a flow rate of 300 $\mu\text{L}/\text{min}$ (gradient 5 % to 90 % ACN, during 45 min). In the present analyzes, atmospheric pressure chemical ionization (APCI) was utilized in positive and negative modes.

The determination of the chemical structure of the products of oxidation was undertaken using RP-UHPLC separation and MS² (tandem mass spectrometry) analyses at the lowest collision cell energy (10 eV). For assessing the presence of C = O in the oxidation products 2,4-dinitrophenylhydrazine (2,4-DNPH) was added to acetonitrile solutions [29,30]. As in previous works [29,30,32,33], we evaluated the presence of hydroxyl (–OH) or hydroperoxyl (–OOH) functional groups in the oxidation products by performing H/D exchange by adding 300 μL of high-purity D₂O to 1 mL of samples. FIA-APCI (+/–)-HRMS and RP-UHPLC-APCI (+/–)-HRMS were employed to analyze these solutions.

3. Results and discussion

3.1. Fuels conversion and production of simple aromatics

A large dataset of oxidation products was collected during the present experiments (Tables S1 and S2). Among them, simple aromatic products were quantified by gas chromatography and a flame ionization detector (GC-FID, Table S1). As shown in Fig. 1, both fuel conversion versus temperature and the mole fractions of toluene (C₇H₈) are similar for the three MCHXs. Furan (C₄H₄O) is produced most abundantly during the oxidation of 3M1CHX, whereas benzene (C₆H₆) is predominantly produced during the oxidation of 4M1CHX. In contrast, 1M1CHX produces the least amounts of both benzene and furan, an important VOC present in the atmosphere [34]. Despite these variations, the differences in the molar fractions of toluene between the three fuels are not significant.

3.2. Formation of complex oxygenated products

Two temperatures (620 and 680 K) were selected for the HRMS analyses. HRMS spectra are provided in Fig. S1. They correspond to the lower temperature of the cool-flame and end of the negative temperature coefficient. More products were observed at 680 K. For that reason, we selected that condition to present most of the results. HRMS analyses of the samples collected in acetonitrile generated a large set of chemical formulas. Whereas the structures corresponding to these chemical formulas could not be obtained exactly, several chemometric tools were employed to obtain a classification of the oxidation products. We calculated oxidation state of carbon, aromaticity index, and aromaticity equivalent index and used Van Krevelen plots to identify chemical classes in the oxidation products. Chemicals containing several O-atoms were detected. As already introduced, H/D exchange using D₂O and reaction with 2,4-DNPH were completed to check the presence of hydroxyl or hydroperoxyl groups, and C = O functional groups in the products of oxidation, respectively.

Oxidation products, including carboxylic acids and carbonyls, were detected. Among these, isomers of C₇H₁₀O₃ were identified. DNPH derivatization confirmed the presence of a carbonyl group in all the eluted isomers detected in the oxidation samples of the MCHX isomers. Furthermore, a signal corresponding to C₇H₉D₁O₃ (C₇H₁₀O₃ + D₂O) confirmed the presence of an OH or OOH functional group in their structure. These compounds were expected to be keto-hydroperoxides KHPs, formed via the second O₂ addition on the fuel radical (Reactions (1)–(5)). Their chromatograms are represented in Figure S2 (Supplementary information). Different isomers are ionized differently in positive and negative ionization modes (Fig. S2). This was systematically tested experimentally. The results are presented in the SM (Table S3). To obtain structural information, we analyzed their MS² spectra. Examples of the obtained MS² spectra are presented in Fig. 2,

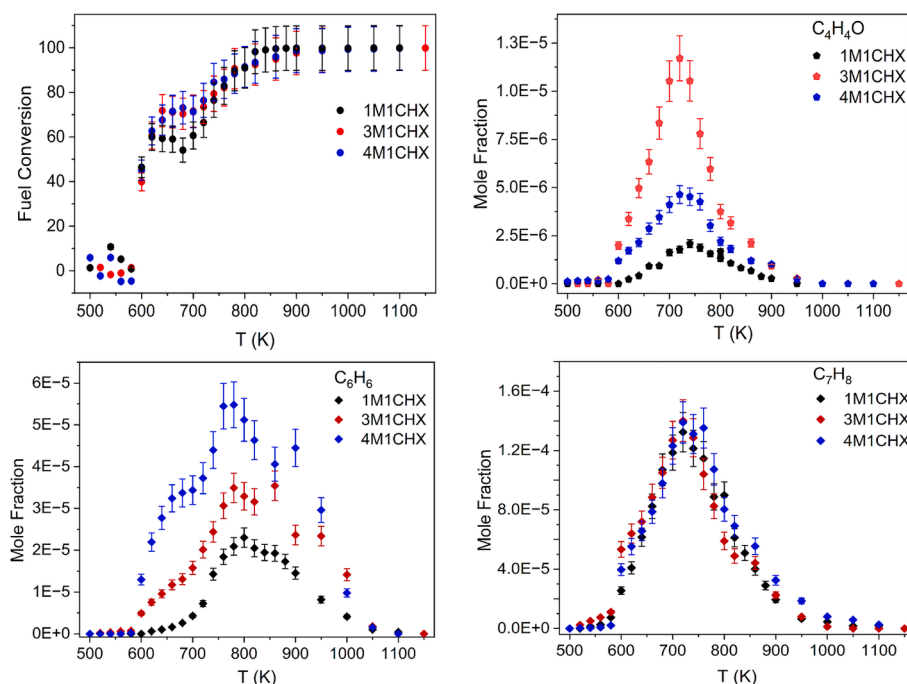


Fig. 1. Conversion of the three fuels versus temperature and mole fractions of simple aromatics obtained by GC-FID (C_4H_4O : furan; C_6H_6 : benzene; C_7H_8 : toluene).

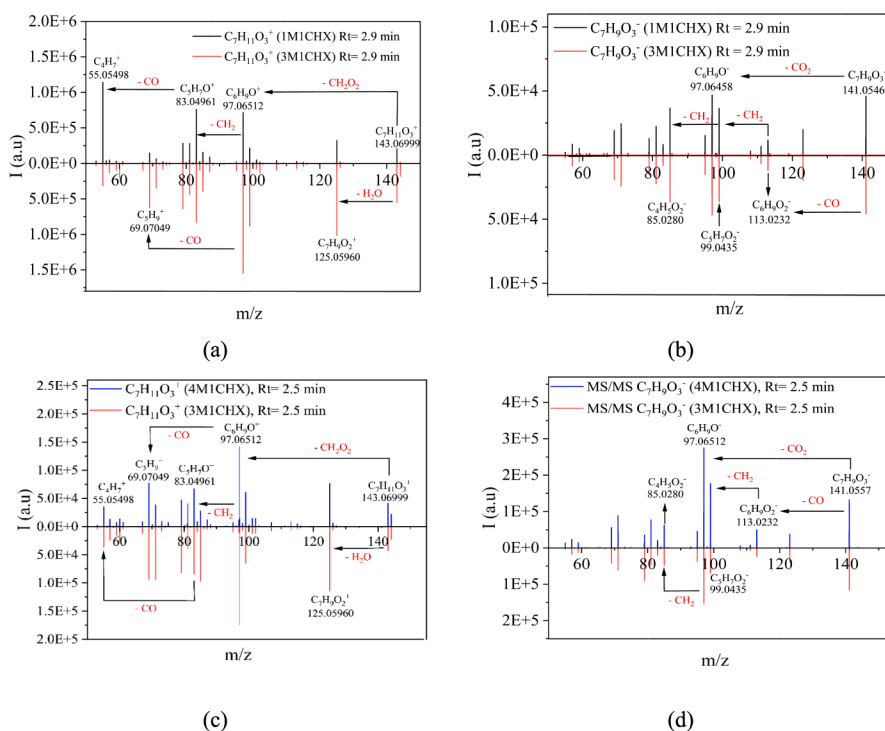


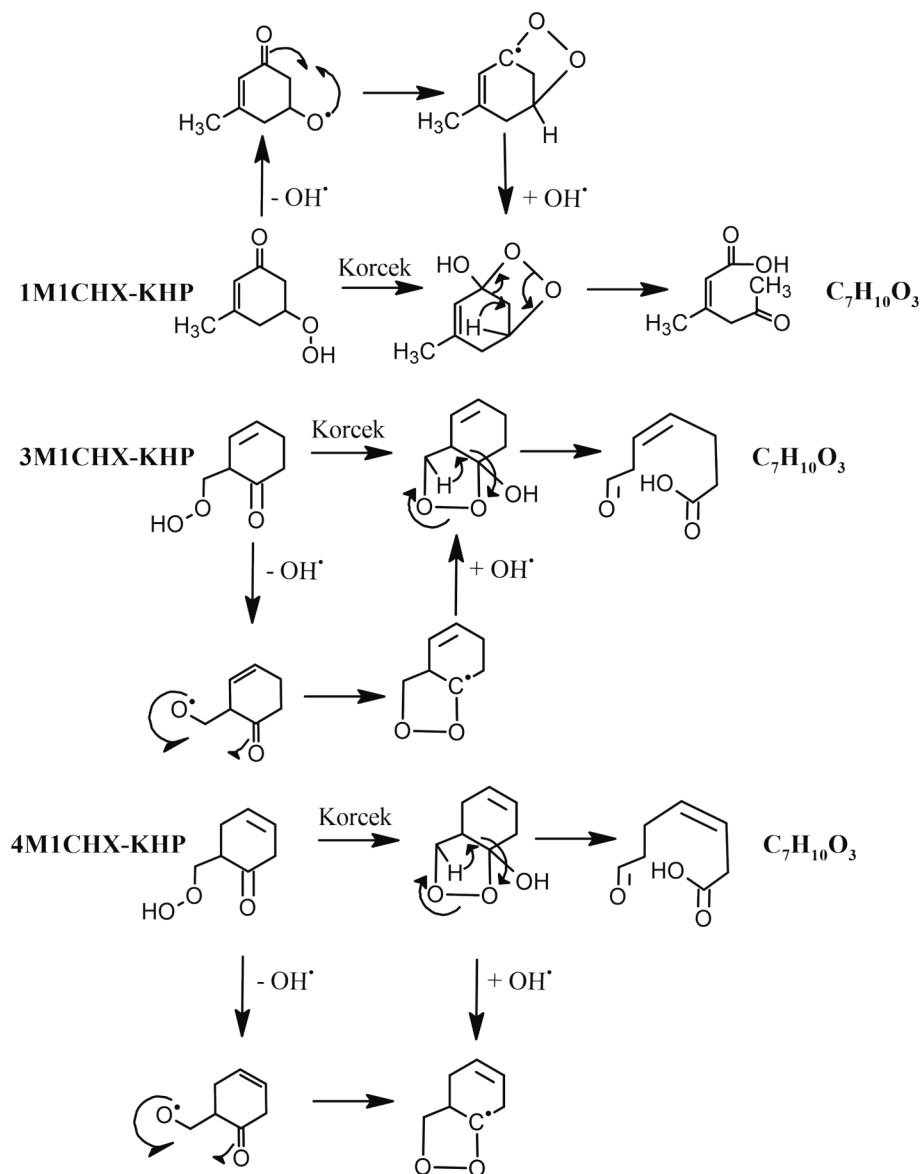
Fig. 2. MS^2 of the $C_7H_{10}O_3$ isomers formed during 1M1CHX, 3M1CHX, and 4M1CHX oxidation at 680 K, ionized with (a) APCI (+), $C_7H_{11}O_3^+$, m/z 143.0699, (b) APCI (-), $C_7H_9O_3^-$, m/z 141.0546, (c) APCI (+) $C_7H_{11}O_3^+$, m/z 143.0699, (d) APCI (-), $C_7H_9O_3^-$, m/z 141.0557.

Fig. S3, and Fig. S4 for $C_7H_{10}O_3$, $C_7H_8O_3$, and $C_7H_{10}O_4$, respectively. The same fragments were observed for all isomers formed during the oxidation of MCHX isomers, but with varying intensities. According to the literature, the presence of fragments corresponding to the loss of CO_2 and CH_2O_2 from parent ions $[M-H]^-$ and $[M+H]^+$, respectively, indicates the presence of carboxylic acids in the molecules [35]. These fragments were detected in the MS^2 spectra of $C_7H_{10}O_3$ isomers in both

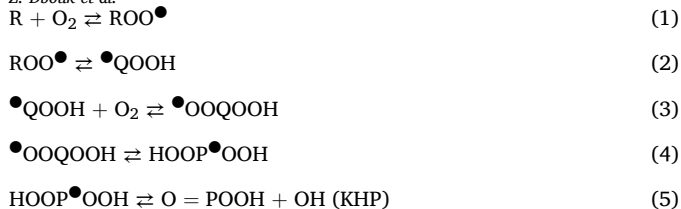
positive and negative modes ($C_6H_9O^+$ and $C_6H_9O^-$), as shown in Fig. 2. Additionally, the presence of fragments formed by the loss of a CO group from the parent ion ($[M+H]^+ / [M-H]^-$) or from other activated fragments (fragments $C_5H_7^+$, $C_4H_7^+$, etc.) indicates that the isomers contain a carbonyl group. The determination of the family of the carbonyl group was not possible. Thus, detected $C_7H_{10}O_3$ isomers were identified as keto-carboxylic acids or aldo-carboxylic acids. Under cool

flame conditions, the Korcek mechanism is often used to explain the formation of these compounds. In this mechanism, γ -KHPs undergo dissociation, resulting in the formation of carboxylic acids and carbonyl compounds ($O = P-OOH \rightarrow R-C = O + R'-COOH$). Due to the cyclic structure of MCHX, other $C_7H_{10}O_3$ isomers containing a carbonyl and a carboxylic acid group are formed after the dissociation of γ -KHPs according to the Korcek mechanism. These isomers could be among those detected in MCHX oxidation samples. In addition, the literature reveals an alternative decomposition pathway for γ -KHPs that predominantly occurs at temperatures above 600 K [36–38]. This pathway involves the unimolecular dissociation of the O-O bond in the hydroperoxyl group. This dissociation leads to the formation of an oxidized organic intermediate, specifically a 5-membered ring, which is also observed in the Korcek mechanism. Later, this intermediate undergoes a decomposition process similar to that described in the Korcek mechanism. As a result, the final products resulting from this decomposition pathway are identical to those predicted by the Korcek mechanism. Scheme 1 illustrates an example of the decomposition of one of the γ -KHP compounds formed during the oxidation of each MCHX isomer in the JSR, according to both the Korcek mechanism and through the unimolecular dissociation of the

O-O bond in the hydroperoxyl function. Similarly, other keto/aldo-carboxylic acids were identified in the MCHX oxidation samples through MS² analysis. Among these were isomers of $C_7H_8O_3$ and $C_7H_{10}O_4$, which were expected to be olefinic KHPs and olefinic dihydroperoxides, respectively. However, based on their MS² spectra, we identified these compounds as keto/aldo-carboxylic acids. Examples of their MS² spectra are shown in Figs. S3 and S4. Moreover, in addition to the previously discussed species, other oxidation products were detected, including diketones ($C_7H_8O_2$), which are produced by the dehydration of KHPs, as well as hydroperoxides ($C_7H_{12}O_2$), formed through the initial addition of O_2 to the fuel radical (Table S2). Additionally, carbonyl compounds ($C_7H_{10}O$) resulting from the dehydration of hydroperoxides ($C_7H_{12}O_2$), such as 3-methyl-2-cyclohexen-1-one, were identified. This isomer was detected in the oxidation samples of all three fuels. It was observed that MCHX isomers share several common isomers of these oxidation products. This similarity may be attributed to isomerization reactions facilitated by the presence of endocyclic double bonds in the fuels, which stabilize the radicals formed during the oxidation process through resonance.



Scheme 1. Decomposition of γ -KHP isomers, potentially formed during MCHX isomer oxidation, via the Korcek mechanism, or through the unimolecular dissociation of the O-O bond in the hydroperoxyl group the leading to $C_7H_{10}O_3$ isomers.



3.3. Chemometric analyses

VK graphs were plotted to characterize the multiplicity of products observed during the oxidation of MCHX isomers at 680 K. These plots were generated using APCI+/- and FIA-HRMS data, as illustrated in Fig. 3. The lines in Fig. 3a indicate the different reaction mechanisms identified in the literature: line 1: hydrogenation, line 2: hydration, line 3: oxidation, line 4: carbonylation, and line 5: carboxylation, or their reverse processes [39,40]. The colors represent the number of oxygen atoms present in the molecule. In this study, we considered species with a maximum of 5 oxygen atoms, an H/C ratio between 0 and 2.8, and an O/C ratio between 0 and 1.5. As can be seen from Fig. 3, on line 1 (hydrogenation/dehydrogenation), for the three isomers, we observe the production of unsaturated compounds (O/C = 0, H/C < 2). For H/C > 0.7 and O/C = 0, the three fuels show a similar distribution of non-oxygenated species, including hydrocarbons (C₇H₁₂) with an H/C ratio of 1.7. For H/C ≤ 0.7, fewer chemical formulas were detected in the case of 3M1CHX, indicating less dehydrogenation at this temperature. The species on line 1 with O/C = 0 could correspond to aromatics and polyaromatics. On line 2 (hydration/dehydration) and 3 (Oxidation/deoxidation), the VK diagrams show similarities among the three hydrocarbons. Between line 4 (carbonylation/decarbonylation) and line 5 (carboxylation/decarboxylation), the number of highly oxygenated products (species with 5 oxygen atoms) is similar across the fuels but slightly lower for 3M1CHX, indicating a comparable degree of oxidation for all three. VK diagrams for products observed during the oxidation of MCHX isomers at T = 620 K were also plotted, they are presented in Figure S5.

Two temperatures (620 and 680 K) were selected to characterize the oxidation of the three MCHX isomers. We plotted the computed oxidation state of carbon (OSc ≈ 2O/C - H/C [16,31]; H, C, and O are the number of hydrogen, carbon, and oxygen atoms, respectively), vs. the number of carbon atoms in chemical formulas (Fig. 4).

Fig. 4a-c show similar trends observed for all fuels, with no significant differences except that 1M1CHX presents more oxidized species with a high number of carbon atoms compared to the other two fuels. The oxidation products of 1M1CHX can form these species through oligomerization [41,42]. The data in the range OSc < 0 and C > 40 confirm the existence of unsaturated or aromatic chemical compounds, which is in line with previous works [43]. The OSc varies as the O/C ratio whereas C-C bonds do not impact the OSc value [24]. For species with OSc in the range of -1.5 < OSc < 0, there are species with the same number of carbon and oxygen atoms but different OSc values. These variations result from dehydrogenation processes, as the H/C ratio is inversely proportional to the OSc value. Multiple dehydrogenation processes can lead to the formation of polyunsaturated, aromatic, and poly-aromatic products. Similarly, there are species with the same number of carbon atoms but different numbers of oxygen atoms. These species have likely undergone oxidation, resulting in highly oxygenated species and an increase in the OSc.

3.4. Polyunsaturated or polyaromatic products of oxidation

To assess the presence of different chemical classes in the products of oxidation, we calculated the modified Aromaticity Index (AI_{mod}) for all detected chemical formulas: AI_{mod} = [1 + C - (0.5 × O) - (0.5 × H)] / [C - (0.5 × O)], with C, H, and O being the number of carbon, hydrogen, and

oxygen atoms, respectively [25,44]. Based on the AI_{mod} value, oxidation products were classified into five chemical classes defined based on previous works [45]: (1) aliphatic compounds (AI_{mod} ≤ 0), (2) olefinic and naphthenic products (0 < AI_{mod} ≤ 0.3), (3) highly unsaturated chemicals (0.3 < AI_{mod} ≤ 0.5), (4) aromatic compounds (0.5 < AI_{mod} ≤ 0.67), and (5) condensed aromatics (0.67 < AI_{mod}). Fig. 5 shows the relative frequencies of all oxidation products obtained during the oxidation of the three hydrocarbons at 680 K. In the histograms shown in Fig. 5, each bar represents the fraction of chemical formulas found in a specific AI_{mod} range. Since only the chemical formulas having signal intensities ≥ 5000 counts, the effect of the variation of ionization cross sections across chemical classes should not be critical. According to this figure, during the oxidation of 1M1CHX in the JSR (3000 ppm, 10 bar, T = 680 K, φ = 0.5, τ = 2 s), the majority of the formed species belong to the olefinic and naphthenic compounds family (38.5 %). In contrast, for 3M1CHX and 4M1CHX, olefinic and naphthenic compounds (33.6 % and 29.4 %, respectively) and aliphatic compounds (33.3 % for 3M1CHX and 31.6 % for 4M1CHX) are produced in almost equal amounts, thus representing the majority of the formed products. For all three fuels, we observed moderate formation of aromatic compounds (9 %, 8.5 %, and 13.2 % for 1M1CHX, 3M1CHX, and 4M1CHX, respectively) as well as polyaromatic compounds (8.9 %, 7.7 %, and 10 % for 1M1CHX, 3M1CHX, and 4M1CHX, respectively). These species are generated in minimal relative quantities and are comparable for all fuels. The same analysis was performed for the products obtained during the oxidation of MCHX isomers at 620 K in the JSR. The relative frequencies of the chemical classes of oxidation products obtained during the oxidation of the three hydrocarbons at 620 K are presented in Figure S6 (Supplementary Information). The results are similar to those obtained at 680 K; the formation of aromatic and poly-aromatic species is also observed. Additionally, as mentioned above, species on the vertical line with O/C = 0 (line 1) in the VK graphs (Fig. 3) could correspond to polyunsaturated hydrocarbons, aromatic, and poly-aromatic species. Among these species, chemical formulas C_nH₄ (n = 4-21, n = 4-22, and n = 4-16 for 1M1CHX, 3M1CHX, and 4M1CHX, respectively) and C_nH₆ (n = 4-19, n = 4-34, and n = 4-7 for 1M1CHX, 3M1CHX, and 4M1CHX, respectively) were observed for all MCHX isomers. To gain further precision about the chemical classes of these species, we zoomed in on the VK diagrams in the region of 0 ≤ O/C ≤ 0.5 and H/C ≤ 1 and calculated the relative frequencies of AI_{mod} for species present in this zone. Fig. 6 illustrates the VK diagrams and the relative frequencies of the chemical classes of these products. Unexpectedly, aliphatic and olefinic/naphthenic classes were absent. The majority of species in this zone correspond to aromatic compounds (48 %, 51 %, and 54 % for 1M1CHX, 3M1CHX, and 4M1CHX, respectively) followed by poly-aromatic compounds (33 %, 39 %, and 37 % for 1M1CHX, 3M1CHX, and 4M1CHX, respectively), and the remaining are highly unsaturated compounds (19 %, 10 %, and 9 % for 1M1CHX, 3M1CHX, and 4M1CHX, respectively).

Whereas computing AI_{mod} allows assessing the presence of aromatic hydrocarbons in the products of oxidation, calculating the aromaticity equivalent index (Xc = [3 (DBE - m × O) - 2] / (DBE - m × O), with m = 1) was claimed to be more useful [26]. Thus, Xc were calculated for the products of oxidation of MCHX isomers. Using this value, all oxygen atoms are considered to form π bonds with carbon atoms. Under this assumption, the quantity of aromatic and poly-aromatic species is underestimated. This approach evaluates the minimal probability of the presence of aromatic species among the oxidation products. The chemical formulas are sorted based on their Xc values. Referring to the work of Zhang et al. [46] and Yassine et al. [26], Xc ≥ 2.5 is considered corresponding to aromatic species, and Xc ≥ 2.7143 to condensed aromatic species. Fig. 7 displays the presently obtained results.

It is observed that during the oxidation of MCHX isomers, numerous aromatic and poly-aromatic species are formed with 0 ≤ H/C < 1.7 and 0 ≤ O/C < 0.5. The distribution of the number of carbon atoms in the aromatic compounds formed during the oxidation of 1M1CHX at T = 680 K ranges from 6 to 28. For those produced during the oxidation of

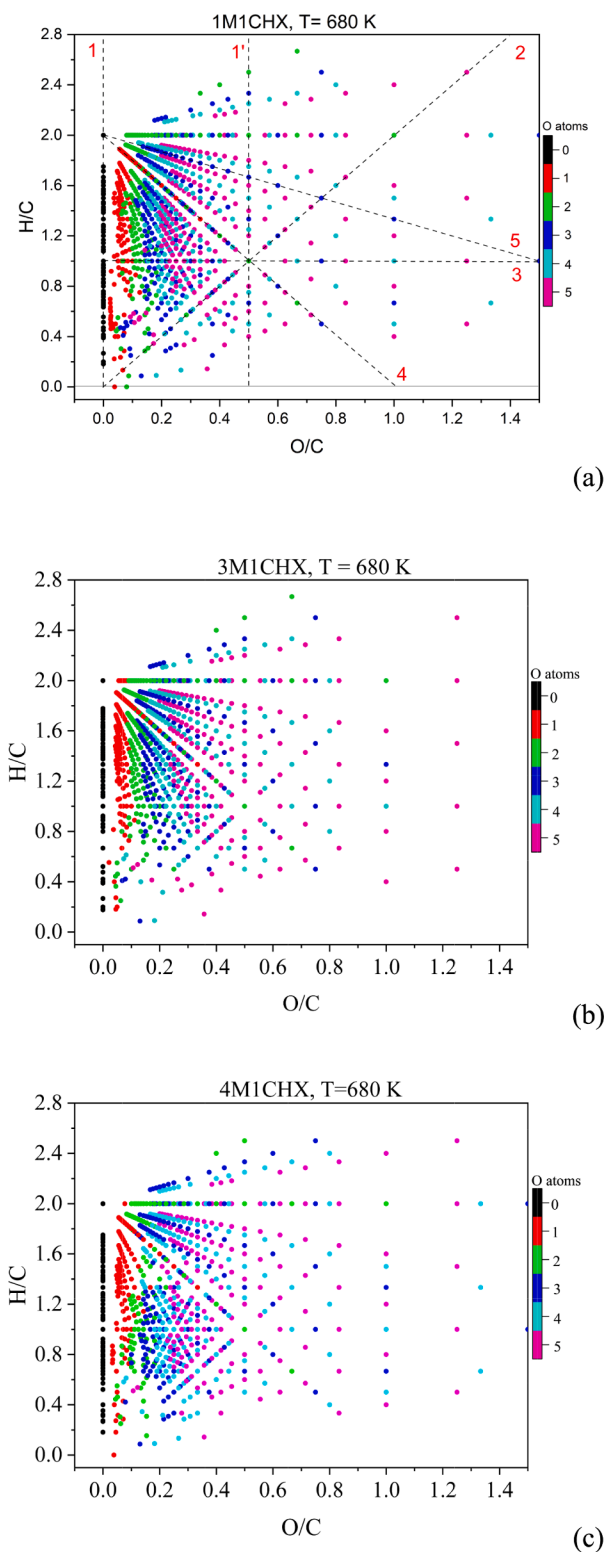
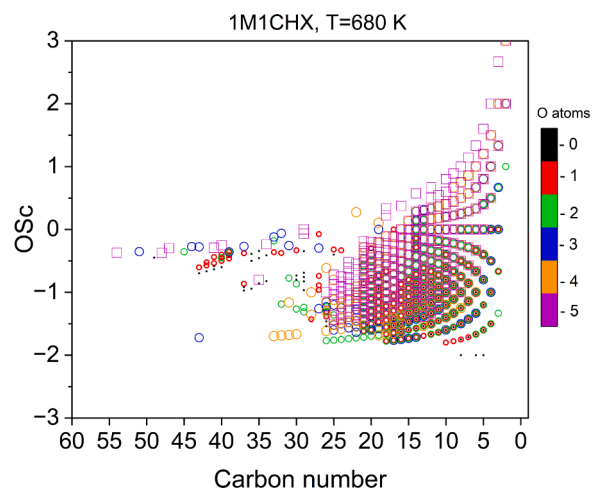


Fig. 3. VK diagrams of oxidation products from (a) 1M1CHX, (b) 3M1CHX, and (c) 4M1CHX with up to 5 oxygen atoms, formed in the JSR (3000 ppm, 10 bar, $T = 680$ K, $\phi = 0.5$, $\tau = 2$ s) and detected by FIA-APCI (+/-)-HRMS. 'O-atoms' indicates the number of oxygen atoms in chemical formulas.

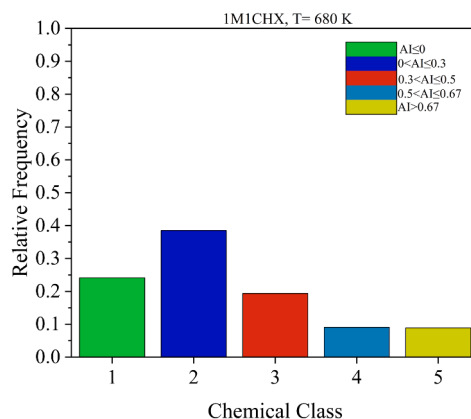
3M1CHX and 4M1CHX, it ranges from 6 to 23 carbon atoms and from 5 to 29 carbon atoms, respectively. Concerning condensed aromatic species, the distribution ranges from 13 to 51 carbon atoms for 1M1CHX, from 13 to 55 carbon atoms for 3M1CHX, and from 11 to 55 carbon atoms for 4M1CHX. Additionally, it is noted that the majority of the products with $O/C = 0$ and $H/C \leq 0.7$ correspond to condensed aromatic

species ($2.7 < X_c \leq 3$). Furthermore, most of the species formed with an O/C value lower than approximately 0.25 correspond to aromatic compounds ($2.5 \leq X_c \leq 2.7$).

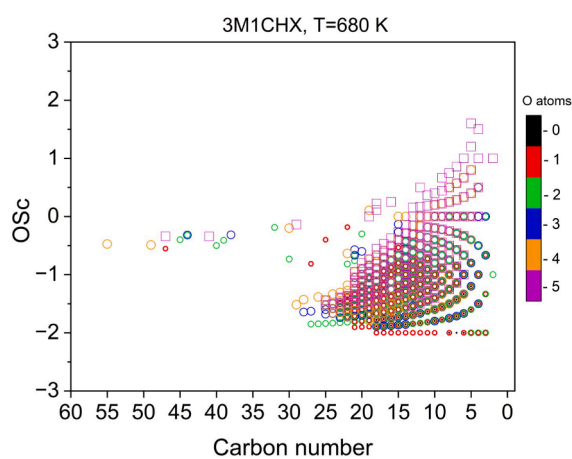
For the products obtained from the oxidation of 1M1CHX in the JSR at 680 K with $2.5 \leq X_c \leq 3$, it is observed that 55.7 % of these products correspond to aromatic compounds, while 44.3 % correspond to



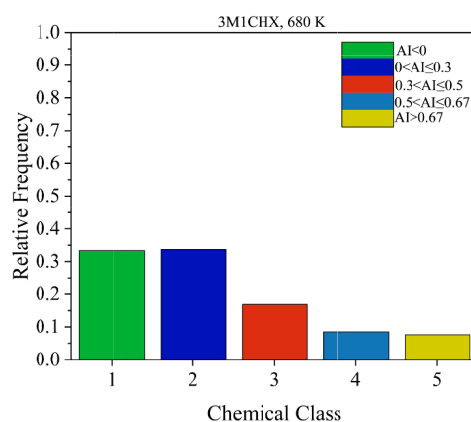
(a)



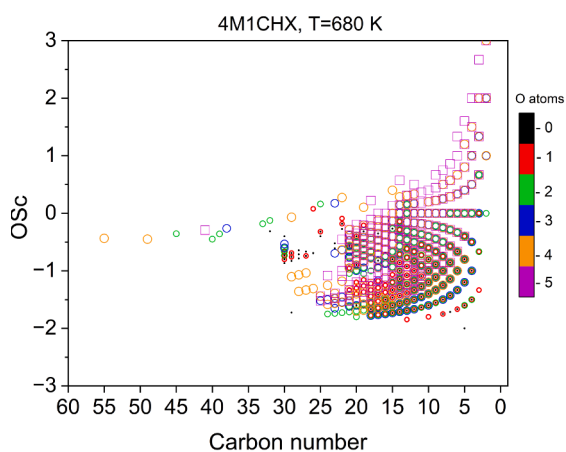
(a)



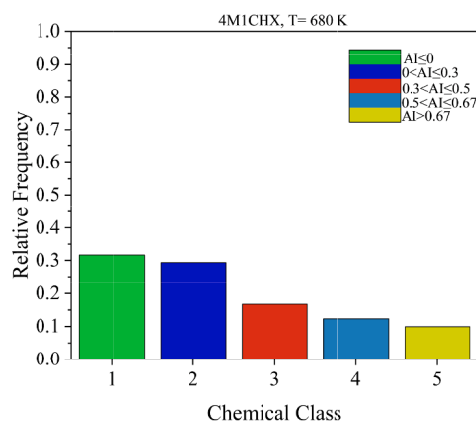
(b)



(b)



(c)



(c)

Fig. 4. Overview of the distribution of MCHXs oxidation products observed by APCI+/-, FIA-HRMS, (a) 1M1CHX, (b) 3M1CHX, and (c) 4M1CHX. The oxidation state of carbon is plotted as a function of the number of C-atoms. The color coding indicates the number of O-atoms in the chemical formulas. Different symbols are used for the different numbers of O-atoms to help the reading. Although soft ionization was used, one cannot exclude some of the detected chemical formulas derive from fragmentation in the ionization source.

Fig. 5. Relative frequencies of the different chemical classes observed during the oxidation of (a) 1M1CHX, (b) 3M1CHX, and (c) 4M1CHX in the JSR (3000 ppm, 10 bar, $T = 680$ K, $\phi = 0.5$, $\tau = 2$ s). APCI+/-, FIA-HRMS data were used for these plots.

condensed aromatic compounds. Conversely, for the products obtained from the oxidation of 3M1CHX under the same conditions, the majority consists of aromatic compounds (66.3 %). In the case of the products obtained from 4M1CHX, there is a very close percentage between simple aromatic compounds (48.1 %) and condensed aromatic compounds (51.9 %).

The formation of aromatics and poly-aromatics under cool flame conditions was also observed in our previous study on the oxidation of

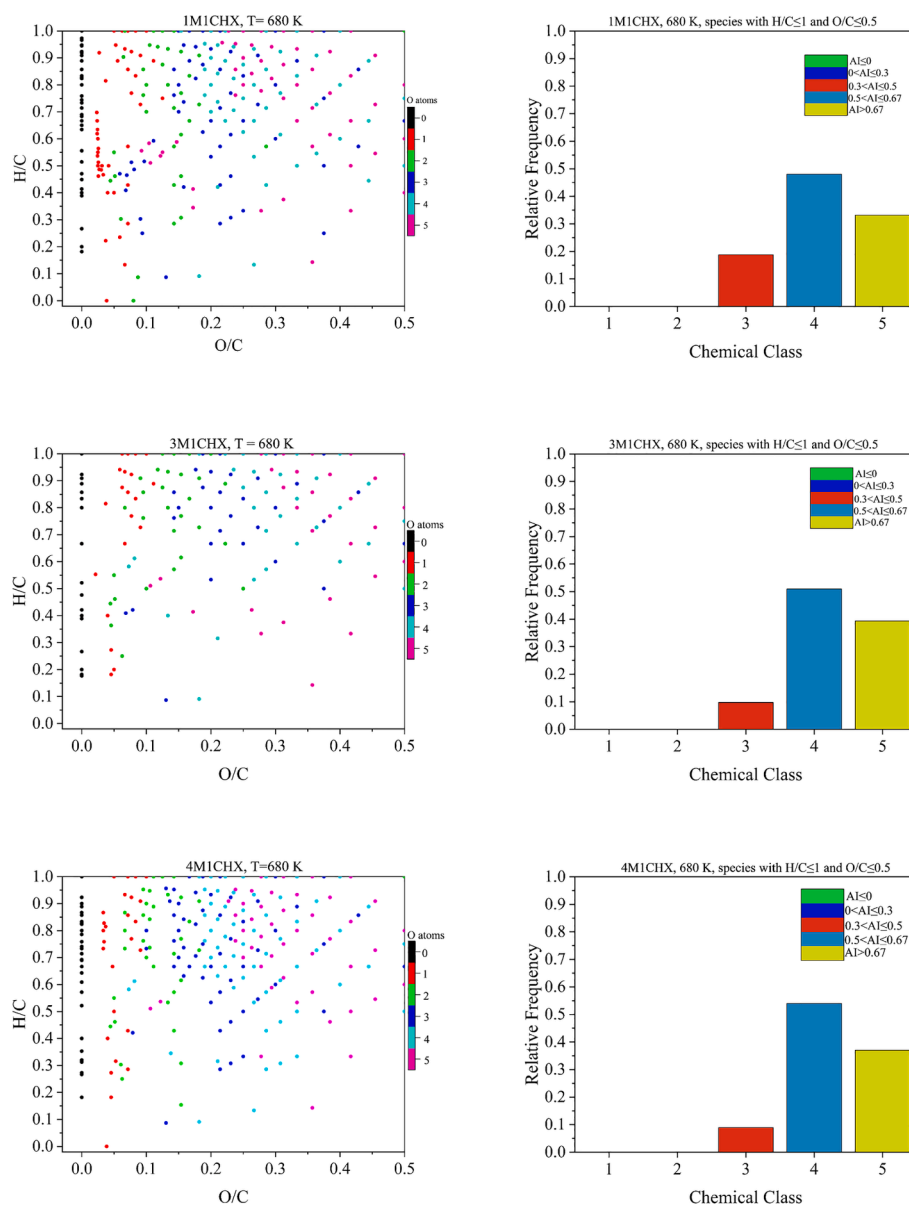


Fig. 6. VK plot for MCHXs oxidation products at 680 K (left) and frequency of occurrence of chemical classes (right). APCI+/-, FIA-HRMS data were used in these plots. Only species with $0 \leq O/C \leq 0.5$ and $H/C \leq 1$ are considered in these plots.

two monoterpenes, i.e., limonene and α -pinene [22]. These compounds have structures similar to the MCHX isomers presented in this work, but they are more complex. The formation of aromatic and poly-aromatic products was not expected under cool flame conditions. It appears that during the oxidation of cyclic alkenes, a similar oxidation mechanism leading to the formation of aromatics occurs. However, no reaction mechanism describing their formation under these conditions has been presented in the literature. Nevertheless, one can propose that it results from successive H-atom abstraction on the fuels, similarly to what was proposed for the formation of benzene from cyclohexane cool-flame in a rapid compression machine [21]. Further investigations are needed, particularly due to their significant environmental impact. This impact is largely attributed to their high persistence, resulting from their chemically stable structures and resistance to biodegradation [47].

4. Conclusions

The oxidation in a JSR under cool flame conditions of three methylenecyclohexene isomers produced a large set of complex oxidation

products detected by HRMS. These products include derivatives from the decomposition of γ -KHPs, which contain both carbonyl and carboxylic acid groups, as well as other oxidation products with similar functional groups. Whereas the formation of benzene has been observed earlier during the oxidation of cyclohexane at 480 °C and 500 Torr and that benzene production was measured during the oxidation of cyclohexane, cyclohexene, and 1,3-cyclohexadiene in a rapid compression machine under stoichiometric cool-flame conditions and elevated pressure (7 to 14 bar), in the present work, the formation of aromatics, polyaromatic hydrocarbons, and polyunsaturated products was observed in cool-flame conditions. The chemical classes of the products were determined using graphic and chemometric tools (VK plots, oxidation state of carbon, aromaticity index, and aromaticity equivalent index). This work, extended from our previous studies on the oxidation of terpenes, further demonstrates the complexity of reaction pathways and chemical products formed under cool flame conditions. Beside the quantitative GC data presented here, usable for kinetic modeling, the other data obtained by HRMS are only qualitative. More work is needed to provide enough data for kinetic modeling.

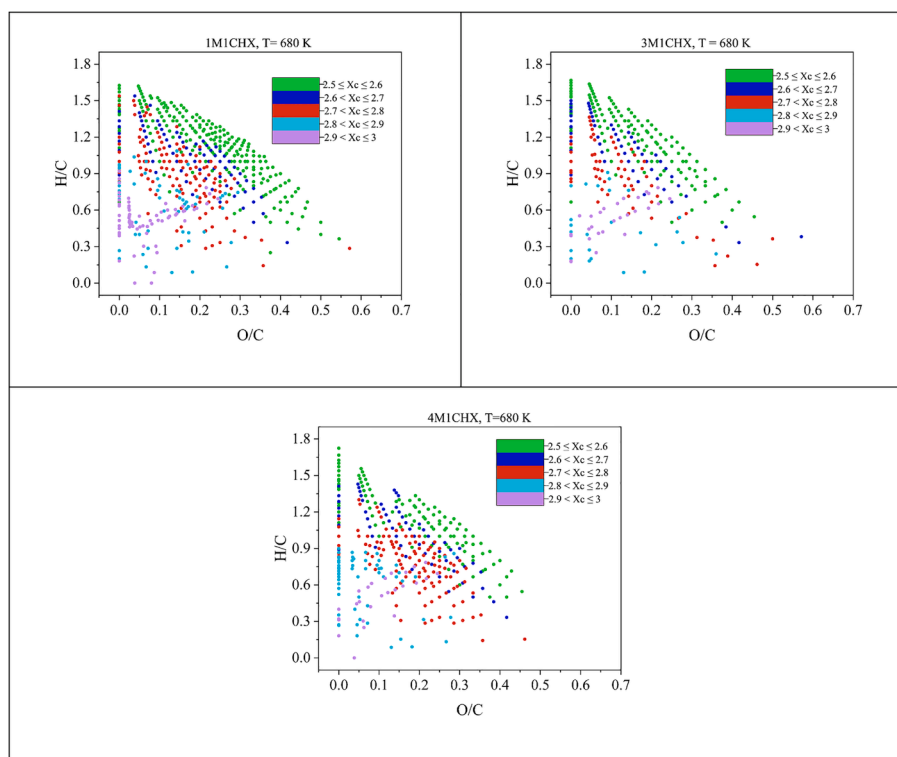


Fig. 7. VK-Xc plot for MCHXs oxidation products. APCI+/-, FIA-HRMS (samples taken at 680 K). Colors are used to indicate the computed Xc ranges.

CRediT authorship contribution statement

Zahraa Dbouk: Writing – review & editing, Writing – original draft, Validation, Methodology, Investigation, Data curation. **Roland Benoit:** Writing – review & editing, Validation, Supervision, Methodology, Data curation, Conceptualization. **Bakr Hoblos:** Writing – review & editing, Validation, Investigation, Data curation. **Nesrine Belhadj:** Writing – review & editing, Validation, Supervision, Investigation. **Philippe Dagaut:** Writing – review & editing, Writing – original draft, Supervision, Resources, Methodology, Funding acquisition, Conceptualization.

Declaration of competing interest

The authors declare that they have no known competing financial interests or personal relationships that could have appeared to influence the work reported in this paper.

Acknowledgements

This work received financial support from the LabEx CAPRYSES (ANR- 11-LABX-006-01) funded by the Programme d'Investissement d'Avenir. ZD and BH received a doctoral grant from the French Ministry of Research and Higher Education (MESRI).

Appendix A. Supplementary material

Supplementary data to this article can be found online at <https://doi.org/10.1016/j.fuel.2024.133644>.

Data availability

Data will be made available on request.

References

- [1] Seinfeld JH, Pandis SN. Atmospheric Chemistry and Physics: From Air Pollution to Climate Change. 2nd ed.; Hoboken, NJ: Wiley-Interscience; 2006. p. 1232.
- [2] Pourbafrani M, Forgács G, Horváth IS, Niklasson C, Taherzadeh MJ. Production of biofuels, limonene and pectin from citrus wastes. *Bioresour Technol* 2010;101:4246–50.
- [3] Harvey BG, Wright ME, Quintana RL. High-density renewable fuels based on the selective dimerization of pinenes. *Energy Fuels* 2010;24:267–73.
- [4] Chetehouna K, Courty L, Mounaim-Rousselle C, Halter F, Garo J-P. Combustion characteristics of p-cymene possibly involved in accelerating forest fires. *Combust Sci Technol* 2013;185:1295–305.
- [5] Courty L, Chetehouna K, Halter F, Foucher F, Garo JP, Mounaim-Rousselle C. Experimental determination of emission and laminar burning speeds of alpha-pinene. *Combust Flame* 2012;159:1385–92.
- [6] Bierkandt T, Hoener M, Gaiser N, Hansen N, Koehler M, Kasper T. Experimental flat flame study of monoterpenes: insights into the combustion kinetics of alpha-pinene, beta-pinene, and myrcene. *Proc Combust Inst* 2021;38:2431–40.
- [7] Zeppieri S, Brezinsky K, Glassman I. Pyrolysis studies of methylcyclohexane and oxidation studies of methylcyclohexane and methylcyclohexane/toluene blends. *Combust Flame* 1997;108:266–86.
- [8] Marchal A. Etude de la contribution des familles chimiques constitutives des gazoles a la formation de polluants non réglementes. Orléans, France: Ph.D., Université d'Orléans; 1997.
- [9] Yang Y, Boehman AL. Experimental study of cyclohexane and methylcyclohexane oxidation at low to intermediate temperature in a motored engine. *Proc Combust Inst* 2009;32:419–26.
- [10] Narayanaswamy K, Pitsch H, Pepiot P. A chemical mechanism for low to high temperature oxidation of methylcyclohexane as a component of transportation fuel surrogates. *Combust Flame* 2015;162:1193–213.
- [11] Liu J, Hu E, Zheng W, Zeng W, Chang Y. A new reduced reaction mechanism of the surrogate fuel for RP-3 kerosene. *Fuel* 2023;331:125781.
- [12] Sakai T, Nakatani T, Takahashi N, Kunugi T. Thermal reactions of 4-vinylcyclohexene, cyclohexene, and 4-methylcyclohexene - Kinetics and mechanism. *Ind Eng Chem Fund* 1972;11:529–33.
- [13] Garnett JL, Johnson WD, Sherwood JE. Pyrolysis of 1-methylcyclohexene and methylenecyclohexane. *Aust J Chem* 1976;29:599–607.
- [14] Tian Z, Zhu S, Li J, Yan Y. Decomposition of 3-methylcyclohexene radicals: Beginning of its mechanism development. *Fuel* 2020;271:117591.
- [15] Gaffney JS, Atkinson R, Pitts JN. Reaction of O(P-3) atoms with toluene and 1-methylcyclohexene. *J Am Chem Soc* 1976;98:1828–32.
- [16] Courtneidge JL, Bush M. Studies relating to the oxidative degradation of natural rubber. The autoxidation of 1-methylcyclohexene: primary product analysis, allylic hydroperoxide isolation, and regiochemistry of the initial events. *J Chem Soc Chem Commun* 1989;17:1227–9.

- [17] Atkinson R, Tuazon EC, Aschmann SM. Products of the gas-phase reactions of a series of 1-alkenes and 1-methylcyclohexene with the OH radical in the presence of NO. *Env Sci Technol* 1995;29:1674–80.
- [18] Kim S, Fioroni GM, Park J-W, Robichaud DJ, Das DD, St John PC, et al. Experimental and theoretical insight into the soot tendencies of the methylcyclohexene isomers. *Proc Combust Inst* 2019;37:1083–90.
- [19] Rissanen MP, Kurtén T, Sipilä M, Thornton JA, Kausiala O, Garmash O, et al. Effects of chemical complexity on the autoxidation mechanisms of endocyclic alkene ozonolysis products: from methylcyclohexenes toward understanding α -pinene. *Chem A Eur J* 2015;119:4633–50.
- [20] Gulati SK, Walker RW. Addition of cyclohexane to slowly reacting H₂-O₂ mixtures at 480 °C. *J Chem Soc, Faraday Trans 2* 1989;85:1799–812.
- [21] Lemaire O, Ribaucour M, Carlier M, Minetti R. The production of benzene in the low-temperature oxidation of cyclohexane, cyclohexene, and cyclohexa-1,3-diene. *Combust Flame* 2001;127:1971–80.
- [22] Dbouk Z, Belhadj N, Lailliau M, Benoit R, Dagaut P. On the autoxidation of terpenes: detection of oxygenated and aromatic products. *Fuel* 2024;358:130306.
- [23] Van Krevelen DW. Graphical-statistical method for the study of structure and reaction processes of coal. *Fuel* 1950;29:269–84.
- [24] Kroll JH, Donahue NM, Jimenez JL, Kessler SH, Canagaratna MR, Wilson KR, et al. Carbon oxidation state as a metric for describing the chemistry of atmospheric organic aerosol. *Nat Chem* 2011;3:133–9.
- [25] Koch BP, Dittmar T. From mass to structure: an aromaticity index for high-resolution mass data of natural organic matter. *Rapid Commun Mass Spectrom* 2016;30:250.
- [26] Yassine MM, Harir M, Dabek-Zlotorzynska E, Schmitt-Kopplin P. Structural characterization of organic aerosol using Fourier transform ion cyclotron resonance mass spectrometry: aromaticity equivalent approach. *Rapid Commun Mass Spectrom* 2014;28:2445–54.
- [27] Dagaut P, Cathonnet M, Rouan JP, Foulatier R, Quilgars A, Boettner JC, et al. A jet-stirred reactor for kinetic studies of homogeneous gas-phase reactions at pressures up to ten atmospheres (≈ 1 MPa). *J Phys E: Sci Instr* 1986;19:207–9.
- [28] Dagaut P, Cathonnet M, Boettner JC. Experimental-study and kinetic modeling of propene oxidation in a jet stirred flow reactor. *J Phys Chem* 1988;92:661–71.
- [29] Belhadj N, Benoit R, Dagaut P, Lailliau M, Serinyel Z, Dayma G. Oxidation of di-n-propyl ether: characterization of low-temperature products. *Proc Combust Inst* 2021;38:337–44.
- [30] Belhadj N, Lailliau M, Benoit R, Dagaut P. Towards a comprehensive characterization of the low-temperature autoxidation of Di-n-butyl ether. *Molecules* 2021;26:7174.
- [31] Hecht ES, Scigelova M, Eliuk S, Makarov A. *Encyclopedia of Analytical Chemistry*. Hoboken, New Jersey, USA: JohnWiley & Sons, Ltd.; 2019. p. 1–40.
- [32] Wang Z, Popolan-Vaida DM, Chen B, Moshammer K, Mohamed SY, Wang H, et al. Unraveling the structure and chemical mechanisms of highly oxygenated intermediates in oxidation of organic compounds. *Proc Natl Acad Sci* 2017;114:13102–7.
- [33] Belhadj N, Benoit R, Dagaut P, Lailliau M. Experimental characterization of n-heptane low-temperature oxidation products including keto-hydroperoxides and highly oxygenated organic molecules (HOMs). *Combust Flame* 2021;224:83–93.
- [34] Romanias MN, Coggon MM, Al Ali F, Burkholder JB, Dagaut P, Decker Z, et al. Emissions and atmospheric chemistry of furanoids from biomass burning: insights from laboratory to atmospheric observations. *ACS Earth Space Chem* 2024;8:857–99.
- [35] Demarque DP, Crotti AEM, Vescechi R, Lopes JLC, Lopes NP. Fragmentation reactions using electrospray ionization mass spectrometry: an important tool for the structural elucidation and characterization of synthetic and natural products. *Nat Prod Rep* 2016;33:432–55.
- [36] Jalan A, Alecu IM, Meana-Paneda R, Aguilera-Iparraguirre J, Yang KR, Merchant SS, et al. New pathways for formation of acids and carbonyl products in low-temperature oxidation: the korcek decomposition of gamma-ketohydroperoxides. *J Am Chem Soc* 2013;135:11100–14.
- [37] Goldsmith CF, Green WH, Klippenstein SJ. Role of O₂ + QOOH in low-temperature ignition of propane. 1. Temperature and pressure dependent rate coefficients. *Chem A Eur J* 2012;116:3325–46.
- [38] Goldsmith CF, Burke MP, Georgievskii Y, Klippenstein SJ. Effect of non-thermal product energy distributions on ketohydroperoxide decomposition kinetics. *Proc Combust Inst* 2015;35:283–90.
- [39] Kim S, Kramer RW, Hatcher PG. Graphical method for analysis of ultrahigh-resolution broadband mass spectra of natural organic matter, the van Krevelen diagram. *Anal Chem* 2003;75:5336–44.
- [40] Bi Y, Wang G, Shi Q, Xu C, Gao J. Compositional changes during hydrodeoxygenation of biomass pyrolysis oil. *Energy Fuels* 2014;28:2571–80.
- [41] Ji Y, Shi Q, Ma X, Gao L, Wang J, Li Y, et al. Elucidating the critical oligomeric steps in secondary organic aerosol and brown carbon formation. *Atmos Chem Phys* 2022;22:7259–71.
- [42] El Hajj O, Hartness SW, Vandergrift GW, Park Y, Glenn CK, Anosike A, et al. Alkylperoxy radicals are responsible for the formation of oxygenated primary organic aerosol. *Sci Adv* 2023;9:eadj2832.
- [43] Wang X, Hayeck N, Brüggemann M, Yao L, Chen H, Zhang C, et al. Chemical characteristics of organic aerosols in shanghai: a study by ultrahigh-performance liquid chromatography coupled with orbitrap mass spectrometry. *J Geophys Res Atmos* 2017;122:11703–22.
- [44] Brege MA, China S, Schum S, Zelenyuk A, Mazzoleni LR. Extreme molecular complexity resulting in a continuum of carbonaceous species in biomass burning tar balls from wildfire smoke. *ACS Earth Space Chem* 2021;5:2729–39.
- [45] Schneider E, Czech H, Popovicheva O, Lüttke H, Schnelle-Kreis J, Khodzher T, et al. Molecular characterization of water-soluble aerosol particle extracts by ultrahigh-resolution mass spectrometry: observation of industrial emissions and an atmospherically aged wildfire plume at lake baikal. *ACS Earth Space Chem* 2022;6:1095–107.
- [46] Zhang Y, Wang K, Tong H, Huang R-J, Hoffmann T. The maximum carbonyl ratio (MCR) as a new index for the structural classification of secondary organic aerosol components. *Rapid Commun Mass Spectrom* 2021;35:e9113.
- [47] Haritash AK, Kaushik CP. Biodegradation aspects of Polycyclic Aromatic Hydrocarbons (PAHs): a review. *J Hazard Mater* 2009;169:1–15.